Influence of cloud properties on satellite total ozone observations

Manuel Antón[1,2] and Diego Loyola[3]

Received 19 July 2010; revised 3 December 2010; accepted 14 December 2010; published 11 February 2011.

[1] Clouds represent one of the most important atmospheric factors that can significantly reduce the accuracy of satellite total ozone column (TOC) data. The influence of clouds on the TOC retrieval from satellites is usually assessed by means of theoretical studies using radiative transfer models. In contrast, few experimental results were found in the literature about the effects of the cloud properties on the differences between satellite TOC data and accurate ground-based measurements. This paper is focused on the study of the joined influence of the cloud properties under different satellite viewing conditions on the TOC data derived from four satellite instruments (GOME/ERS-2, GOME-2/MetOp-A, SCIAMACHY/Envisat, and OMI/Aura) using as reference five Brewer spectrophotometers in the Iberian Peninsula. Satellite TOC data under cloud-free and cloudy conditions are compared with ground-based measurements for the time period 2006 to 2009. The TOC products derived using the Differential Optical Absorption Spectroscopy (DOAS) technique, GOME, GOME-2, SCIAMACHY and OMI-DOAS, show a notable underestimation for cloudy conditions that clearly decreases with increasing Sun zenith angles (SZA). For those DOAS TOC products, the viewing zenith angle (VZA) also shows a significant influence on the satellite-Brewer differences, mainly for the west pixels and cloud-free conditions. The OMI-TOMS TOC product under cloud-free and cloudy conditions presents a more stable pattern for both SZA and VZA values, but this result must be interpreted carefully because OMI-TOMS classifies an unrealistic high number of scenes as cloud-free (~57% of all). The analysis of the relative TOC differences as a function of the satellite cloud fraction indicates that SCIAMACHY and OMI-DOAS products have a large difference between the curves corresponding to low and high SZA cases. The two GOME algorithms and, mainly, the OMI-TOMS algorithm present a remarkable stability for all cloud conditions.

Citation: Antón, M., and D. Loyola (2011), Influence of cloud properties on satellite total ozone observations, *J. Geophys. Res.*, *116*, D03208, doi:10.1029/2010JD014780.

1. Introduction

[2] The atmospheric ozone is a crucial trace gas for life on Earth since it protects the living organisms from the harmful effects of ultraviolet irradiation. In addition, the ozone layer plays an important role in global weather and climate [*World Meteorological Organization* (*WMO*), 2006]. Depletion of the ozone layer is a great threat to the human society. Fortunately, stratospheric ozone is expected to recover toward pre-1980s levels in a near future due to the successful implementation of the Montreal Protocol and its Amendments for the reduction of ozone depleting substances. This international treat has also helped prevent significant regional climate change [*Morgenstern et al.*, 2008], and it could phase down the production and consumption of hydrofluorocarbons (HFCs) with high global warming potential [*Molina et al.*, 2009].

[3] Ground-based networks (Dobson, Brewer, SAOZ) have been established to measure the magnitude of the total ozone changes and monitor their long- and short-term trends [*Komhyr*, 1980; *Basher*, 1982; *Kerr et al.*, 1984; *WMO*, 1996]. In addition, several satellite instruments have been launched to derive ozone and other trace gases in the atmosphere from the measurement of the backscattered ultraviolet (UV) solar radiation [*McPeters et al.*, 1998; *Bovensmann et al.*, 1999; *Burrows et al.*, 1999; *Levelt et al.*, 2006; *Munro et al.*, 2006]. These satellite observations have global coverage, which is an important advantage over the ground-based ozone measurements from a sparse network of unevenly distributed stations. The current accuracy of the total ozone columns retrieved by UV-type satellite instruments is, in average, very high (within a few percent) [*Fioletov et al.*, 2002; *Bramstedt et al.*, 2003; *Balis et al.*, 2007a, 2007b; *Lerot et al.*, 2009; *Antón et al.*, 2010]. Nevertheless, to achieve this accuracy, several algorithm corrections are required in the satellite retrievals. One of the

[1]Centro Andaluz de Medioambiente, Universidad de Granada, Granada, Spain.
[2]Departamento de Física Aplicada, Universidad de Granada, Granada, Spain.
[3]Remote Sensing Technology Institute, German Aerospace Center, Wessling, Germany.

0148-0227/11/2010JD014780

most important ones is the cloud correction since the field-of-view of these instruments is relative wide, and clouds are present very often [*Krijger et al.*, 2007].

[4] The physics of cloud influences on the ozone retrieval is well understood, and it is generally divided in three different contributions [*Liu et al.*, 2004; *Kokhanovsky and Rozanov*, 2008; *Stammes et al.*, 2008]: (1) the albedo effect associated with the enhancement of the reflectivity for cloudy scenes compared to cloud-free sky scenes, (2) the increased in-cloud absorption effect relate to the multiple scattering inside clouds which leads to an enhancement of the optical path length, and (3) the so-called shielding effect due to fact that part of the ozone column below clouds is hidden by them. The first two effects produce the overestimation of total ozone column (TOC) because of the apparent increase of the depth of ozone absorption bands. The third effect has an opposite sign since it leads to the underestimation of the TOC data. Therefore, the presence of clouds must be taken into account for accurate satellite TOC retrievals.

[5] Several papers have quantified theoretically using radiative transfer modeling the influence of errors in cloud parameters on the retrieved ozone column, showing that this influence is very dependent of the particular algorithm used in the ozone retrieval [*Koelemeijer and Stammes*, 1999; *Newchurch et al.*, 2001; *Liu et al.*, 2004; *Ahmad et al.*, 2004; *Van Roozendael et al.*, 2006; *Kokhanovsky et al.*, 2007]. These papers show that the cloud fraction (CF), cloud top albedo (CTA), and cloud top pressure (CTP) are the most important quantities for cloud correction on satellite ozone retrievals. However, there are only a few papers in the literature that systematically analyze the influence of these cloud properties on the differences between the satellite and the ground-based TOC measurements. The published studies are usually focused on the analysis of the influence of the satellite reflectivity [e.g., *McPeters et al.*, 2008; *Antón et al.*, 2010] and the CF parameter [e.g., *Balis et al.*, 2007b; *Antón et al.*, 2008, 2009a, 2009b] on the satellite–ground-based differences. The combined effects of the cloud parameters (CF, CTA and CTP) over the satellite–ground-based differences, to our knowledge, have not been yet evaluated systematically and in detail.

[6] The aim of this paper is to study the influence of the three cloud parameters (CF, CTA and CTP) on the TOC data derived from all currently active UV/VIS nadir-viewing satellite instruments using as reference five well-calibrated and well-maintained Brewer spectrophotometers in the Iberian Peninsula. This work is expected to contribute to improve the understanding of satellite TOC observations under cloudy conditions.

[7] The instrumentation and the data used in this paper are described in section 2. Section 3 describes the methodology followed in the analysis. Section 4 presents and discusses the results obtained and, finally, section 5 summarizes the main conclusions.

2. Total Ozone Data

2.1. Satellite Observations

[8] The ESA Global Ozone Monitoring Experiment (GOME) on board the Second European Sensing Satellite (ERS-2) has been recording global measurements of total ozone column since July 1995 [*Burrows et al.*, 1999]. Global coverage at the Equator is achieved with GOME/ERS-2 within three days. The ground swath (960 km) is divided into three ground pixels of 320 km (across orbit) × 40 km (along orbit). The successor instrument, the GOME-2, was launched on board EUMETSAT Meteorological Operational satellite program (MetOp-A) in October 2006. GOME-2/MetOp-A is an enhanced version of GOME/ERS-2 with 4 times higher spatial resolution (80 km × 40 km) and 2 times larger swath (1920 km) resulting in an improved temporal coverage (daily near global coverage at the Equator). The operational algorithm for the retrieval of total ozone column from the GOME/ERS-2 and the GOME-2/MetOp-A is the GOME Data Processor (GDP), which has undergone several years of progressive improvement since its first release in 1995 [*Rodriguez et al.*, 2007; *Spurr et al.*, 2005; *Van Roozendael et al.*, 2006; *Loyola et al.*, 2011]. The GDP algorithm has two main steps to derive the total ozone column: the Differential Optical Absorption Spectroscopy (DOAS) least squares fitting for the ozone slant column, followed by the computation of a suitable Air Mass Factor (AMF) to make the conversion to the vertical column density. The current version 4.4 of the GDP includes two algorithms for the treatment of clouds [*Loyola et al.*, 2007]. The OCRA algorithm derives the cloud fraction from the broadband polarization measurements, while the ROCINN algorithm derives the cloud top height and cloud top albedo from the reflectivity in and around the Oxygen A band. In addition, this new GDP version discriminates between clouds and Sun glint, and incorporates corrections for intracloud ozone and scan angle dependencies [*Loyola et al.*, 2011].

[9] The Scanning Imaging Absorption spectroMeter for Atmospheric CartograpHY (SCIAMACHY) was launched in March 2002 aboard the European platform ENVISAT. SCIAMACHY has a total swath width of 960 km and it provides global coverage in approximately six days at the equator with a typical spatial resolution in nadir of 60 km across track by 30 km along track [*Bovensmann et al.*, 1999]. The SCIAMACHY Ground Processor (SGP) Version 5.0 is the current operational algorithm for the retrieval of total ozone column from this satellite instrument, which is based on the version 4.0 of the GDP. More details about this algorithm can also be found in the work of *Lerot et al.* [2009]. In the present paper we don't use the operational SCIAMACHY products. We use instead SCIAMACHY data processed with the same DOAS/AMF algorithms as GDP 4.0, but for comparison purposes the treatment of clouds is done with the FRESCO+ algorithm [*Wang et al.*, 2008]. In FRESCO+, the cloud top albedo is assumed to have a fixed value of 0.8, and the so-called "effective" cloud top height (pressure) and "effective" cloud fraction are fitted using reflectances in and around the Oxygen A band.

[10] The OMI satellite instrument is on board the NASA EOS-Aura satellite platform launched in July 2004 [*Levelt et al.*, 2006]. This instrument has a 2600 km wide viewing swath such that it is capable of daily, global contiguous mapping of total ozone column with a high spatial resolution of 13 km × 24 km at nadir. The OMI total ozone column data used in this work were obtained from two different algorithms. On the one hand, the OMI-TOMS algorithm (Version 8.5) based on the long-standing NASA TOMS V8 retrieval algorithm [*Bhartia and Wellemeyer*, 2002], which

Table 1. Cloud Retrieval Algorithms Used by the Satellite Data Sets Analyzed in This Work

Data Set	Cloud Fraction	Cloud Top Pressure	Cloud Top Albedo
GOME-2/MetOp-A	OCRA algorithm	ROCINN algorithm	ROCINN algorithm
GOME/ERS-2	OCRA algorithm	ROCINN algorithm	ROCINN algorithm
SCIAMACHY	FRESCO+ algorithm	FRESCO+ algorithm	Fixed value of 0.8
OMI-DOAS	RRS algorithm	RRS algorithm	Fixed value of 0.8
OMI-TOMS	O_2–O_2 algorithm	O_2–O_2 algorithm	Fixed value of 0.8

has been used to process data from a series of four TOMS instruments flown since November 1978. This algorithm uses measurements at four discrete 0.45 nm wide wavelength bands centered at 313, 318, 331 and 360 nm. On the other hand, OMI-DOAS algorithm [*Veefkind et al.*, 2006] is based on the DOAS technique which uses 25 OMI measurements in the wavelength range 331.1 nm to 336.6 nm. Two different methods are used to correct the ozone retrievals for the presence of clouds: the absorption by O_2–O_2 used in OMI-TOMS, and the rotational Raman scattering (RRS) used in OMI-DOAS. As explained by *Stammes et al.* [2008], the two OMI cloud algorithms are based on the determination of the mean photon path in the UV-visible from analysis of spectral features. However, each cloud algorithm uses a different physical process: the first algorithm uses the 477 nm absorption line of O_2–O_2 (collision induced absorption by oxygen), whereas the RRS algorithm uses the filling-in of Fraunhofer lines in the UV due to rotational Raman scattering by air molecules. Finally, both cloud algorithms are based on a simplified Lambertian cloud model with a fixed albedo 0.8, producing two parameters: effective (or radiative) cloud fraction and cloud pressure. In this work, both OMI-TOMS and OMI-DOAS total ozone products are obtained in the new version of the OMI level 1B (radiance and irradiance) data set named collection 3. The works of *Kroon et al.* [2008], *Balis et al.* [2007b] and *Antón et al.* [2009b] analyzed in detail the similarities and differences between OMI-TOMS and OMI-DOAS total ozone column data.

[11] Table 1 summarizes the cloud algorithms used by each satellite data set for deriving the three cloud parameters utilized in this work (CF, CTP and CTA).

2.2. Ground-Based Measurements

[12] The ground-based total ozone data used in this work are obtained from five Brewer spectrophotometers located from north to south at: A Coruña (43.33°N, 8.42°W), Zaragoza (41.01°N, 1.01°W), Madrid (40.45°N, 3.72°W), Murcia (38.03°N, 1.17°W) and El Arenosillo (37.06°N, 6.44°W). These five instruments belong to the Spanish Brewer Network which is managed by the Spanish Agency of Meteorology (AEMET). The main advantage of using a dense local ground-based network is that all instruments follow the same protocol of calibration. In this regard, the Spanish Brewer Network possesses an excellent maintenance record. All instruments of this network are biannually calibrated at El Arenosillo station by comparison with the traveling references Brewer 017 from the International Ozone Services (IOS) and Brewer 185 from the Regional Brewer Calibration Centre-Europe (RBCC-E) [*Redondas et al.*, 2002, 2008]. In this way the ozone calibration of the Spanish Brewer spectrophotometers is traceable to the triad of international reference Brewers maintained by the Meteorological Service of Canada (MSC) at Toronto [*Fioletov et al.*, 2005]. Therefore as the Brewer instruments of the Spanish Network are properly calibrated and regularly maintained, the TOC records derived from Direct Sun (DS) measurements may potentially maintain a relative accuracy of 1% over long time series [*Basher*, 1982; *WMO*, 1996].

[13] The Brewer instruments rely on the method of differential absorption in the Huggins band where ozone presents a strong absorption in the ultraviolet part of the solar spectrum. This method has been broadly described by several reference papers [e.g., *Dobson*, 1957; *Komhyr*, 1980; *Basher*, 1982; *Kerr*, 2002].

3. Methodology

[14] The ground-based TOC data selected for the comparisons are only based on records of DS measurements which are the most accurate TOC data measured from Brewer spectrophotometers. Under cloudiness conditions, the Brewer spectrophotometers do not record direct Sun measurement while the satellite makes the corresponding observation on a cloudy pixel. The Brewer measurements are recorded before or after these conditions, only during cloud-free cases every day. Thus, the use of daily averaged ground-based TOC data instead of, for example, hourly averaged data centered on the satellite overpass allows to significantly increase the number of satellite-Brewer data pairs in the analysis. The use of daily averages is justified because on the average there is not a significant daily TOC variability over the middle latitudes. In addition, uses of daily average Brewer data also allow comparison of the same ground-based measurements with the different satellite observations.

[15] Satellite overpass is selected such that the distance between the center of the satellite pixel and the location of the ground-based stations is always less than 200 km for GOME/ERS-2, GOME-2/MetOp-A and SCIAMACHY instruments, with a median value of 85 km, 23 km and 58 km, respectively. The distance is selected to be smaller than 60 km for OMI instrument (median value of 10 km). In this work, when several satellite pixels comply with the overpass criteria for a given day, only the closest pixel to each ground-based station is considered.

[16] The OMI Science Team has reported that the OMI instrument has developed several row anomalies during the period 2007–2009 which significantly affect to the TOC data for a limited number of satellite cross-track positions (http://www.knmi.nl/omi/research/operations/index.php). All these OMI anomalies have been excluded in this work.

Table 2. The Number of Pairs of Ground-Based–Satellite Data Corresponding to All, Cloud-Free, and Cloudy Conditions[a]

		Cloud-Free Cases		Cloudy Cases	
	All Cases	Criteria	Number	Criteria	Number
GOME-2/MetOp-A	4009	CF = 0%	1640 (40.9%)	CF > 50%	733 (18.3%)
GOME/ERS-2	2409	CF < 5%	700 (29.1%)	CF > 50%	380 (15.8%)
SCIAMACHY	3025	CF < 5%	523 (17.3%)	CF > 50%	529 (17.5%)
OMI -DOAS	4095	CF < 5%	669 (16.3%)	CF > 50%	671 (16.4%)
OMI -TOMS	4095	CF = 0%	2324 (56.7%)	CF > 50%	717 (17.5%)
Combined OMI-DOAS, OMI_TOMS	4095	$CF^{DOAS} < 5\%$ $CF^{TOMS} = 0\%$	660 (16.1%)	$CF^{DOAS} > 50\%$ $CF^{TOMS} > 50\%$	618 (15.1%)

[a]The percentages of cloud-free and cloudy cases with respect to all cases are shown in parentheses.

[17] The relative differences between the daily Brewer (Bre) TOC measurements and the satellite TOC observations (Sat) were calculated for each station using the following expression:

$$RD_i = 100 \times \frac{Sat_i - Bre_i}{Bre_i}.$$

Time series of both satellite and ground-based TOC data extend from January 2007 to December 2009 for GOME-2/MetOp-A and OMI instruments, and from January 2006 to December 2009 for GOME/ERS-2 and SCIAMACHY instruments. The reason of adding one year more for the last two instruments is to increase the number of TOC data in the analysis since they do not provide daily data as it is the case for GOME-2/MetOp-A and OMI instruments. Table 2 shows the number of pairs of ground-based–satellite data used in this work corresponding to all, cloud-free, and cloudy conditions. It can be seen that the number of pairs of data selected for each satellite instrument is different, although there are common cases shared by all data sets (the selected days are exactly the same only for the two OMI data sets). Therefore the influence of daily changing factors (e.g., stratospheric temperature variations, aerosol variability) over the ozone retrievals is not the same for the four instruments. Nevertheless, these factors have a more limited effect than the parameters studied in this work (cloud properties and viewing geometry) and their impact on the results shown in this work is negligible.

[18] Table 2 also shows the CF thresholds used to select cloud-free and cloudy cases. For the two OMI algorithms, identical criteria are used in order to work with the same data set. For cloud-free cases, we choose those measurements that comply at the same time with $CF^{TOMS} = 0\%$ and $CF^{DOAS} < 5\%$. The threshold for OMI-DOAS is slightly higher than for OMI-TOMS since the number of cases with $CF^{DOAS} = 0\%$ is smaller (~4%) compared with $CF^{TOMS} = 0\%$ (~57%). For cloudy cases, the criterion is $CF^{TOMS} > 50\%$ and $CF^{DOAS} > 50\%$. The cloud-free and cloudy criteria for GOME-2/MetOp-A instrument are $CF^{GOME\text{-}2} = 0\%$ and $CF^{GOME\text{-}2} > 50\%$, respectively. GOME/ERS-2 and SCIAMACHY instruments use the some criterion for cloudy cases, $CF^{GOME\text{-}1} > 50\%$, and $CF^{SCIAMACHY} > 50\%$, but the threshold for selecting cloud-free conditions must be slightly increased in order to have a sufficient number of data ($CF^{GOME\text{-}1} < 5\%$, and $CF^{SCIAMACHY} < 5\%$). The percentages of cloud-free cases selected present very different values: 16% for combined OMI-TOMS and OMI-DOAS, 17% for SCIAMACHY, 29% for GOME/ERS-2, and 41% for GOME-2/MetOp-A. In contrast, the cloudy cases show similar percentages, between 16% and 18% for all algorithms.

4. Results and Discussion

[19] The viewing geometry of the satellite measurements changes strongly over the covered ground path and it is described by the satellite solar zenith angles (SZA), viewing zenith angles (VZA) and relative azimuth angle. It is well known that it is necessary to analyze the dependence of the relative differences between satellite and ground-based ozone data with respect to the most relevant viewing geometry because the results obtained using all data simultaneously could be affected by the compensation of cases with opposite viewing conditions [*Antón et al.*, 2008, 2009b, 2010].

[20] In the same way the cloudiness conditions of the satellite measurements show large variations. Table 3 reports the average values of the satellite cloud parameters (cloud fraction, cloud top pressure and cloud top albedo) used in this work. While lower CF averages correspond to GOME-2 (~21%) and OMI-TOMS (~19%) due to the high percentage of cloud-free cases selected by these two satellite data sets, the SCIAMACHY has the larger CF averages (27%). It is interesting to note that the average value of the CTA parameter for both GOME instruments is very similar (~0.55), whereas the two OMI and the SCIAMACHY algorithms work with a fixed CTA of 0.8.

[21] Figure 1 shows the median value of the relative differences between ground-based and five satellite TOC data sets (hereafter called GOME-2, GOME-1, SCIAMACHY, OMI-DOAS, and OMI-TOMS) as a function of the satellite SZA, and using five-degree bins. Each plot shows three curves corresponding to all, cloud-free, and cloudy conditions. Generally speaking, Figure 1 shows that the four DOAS algorithms (GOME-2, GOME-1, SCIAMACHY,

Table 3. The Average Values of the Cloud Fraction (CF), Cloud Top Pressure (CTP), and Cloud Top Albedo (CTA)[a]

	CF (%)	CTP (mbar)	CTA
GOME-2/MetOp-A	21 ± 31	702 ± 170	0.56 ± 0.15
GOME/ERS-2	24 ± 26	713 ± 144	0.55 ± 0.14
SCIAMACHY	27 ± 25	769 ± 188	0.80
OMI-DOAS	24 ± 26	778 ± 175	0.80
OMI-TOMS	19 ± 29	644 ± 169	0.80

[a]The errors correspond with 1 standard deviation.

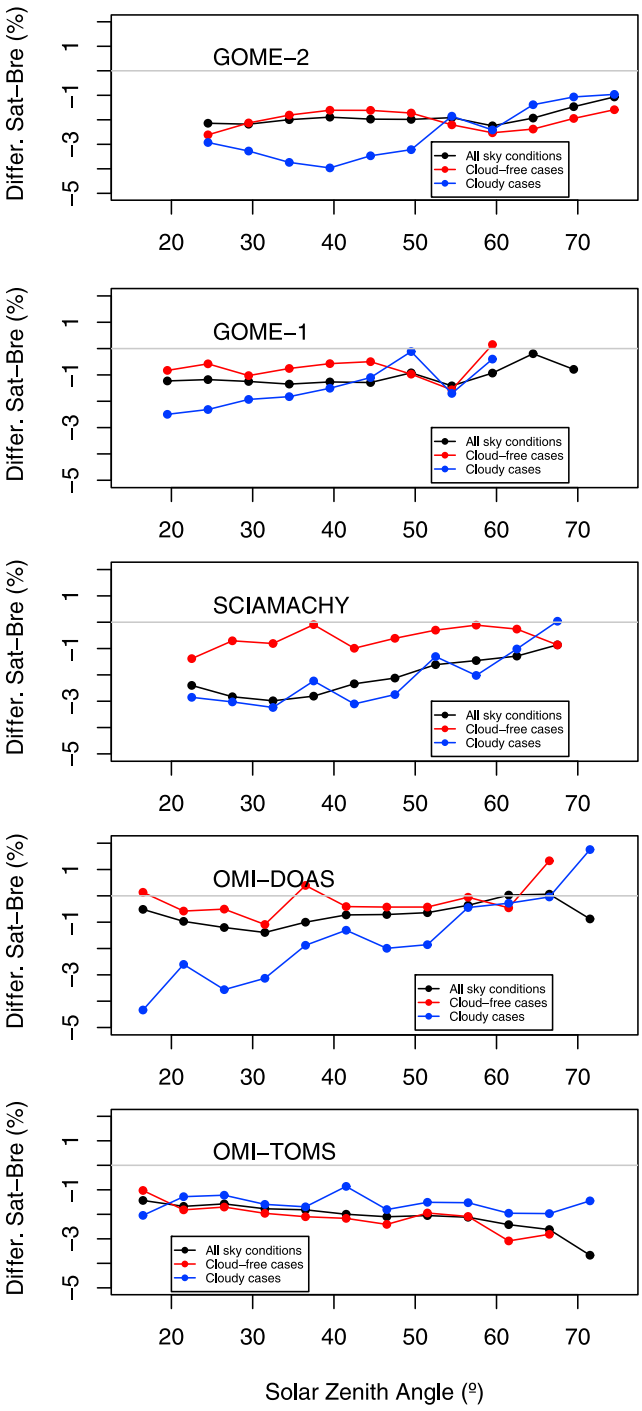

Figure 1. Evolution of the differences between total ozone column data retrieved by satellite (from top to bottom: GOME-2, GOME-1, SCIAMACHY, OMI-DOAS, and OMI-TOMS) and Brewer total ozone column data as function of solar zenith angle for all, cloud-free, and cloudy conditions.

and OMI-DOAS) have, as expected, overall relative differences smaller for cloud-free cases than for cloudy conditions. The OMI-TOMS algorithm shows a different behavior with relative differences slightly larger for cloud-free cases than for cloudy days. This fact is not related to the misclassification of pixels since the relative differences shown in Figure 1 for both OMI algorithms correspond to common pixels.

[22] Analyzing the plots from Figure 1 from top to bottom, we conclude that GOME-2 presents a dependence on SZA for cloudy cases; the relative differences vary from almost −3.5% for low SZA to −1% for large SZA. In contrast, the curve of GOME-2 for the cloud-free cases and all conditions show no significant dependence on SZA. A very similar behavior is observed for GOME-1, SCIAMACHY and OMI-DOAS algorithms. Nevertheless, these last two algorithms show a larger difference between the curves corresponding to cloud-free and cloudy conditions suggesting a possible systematic problem when effective cloud parameters are used in the retrieval. It is important to note the large variation that experiences the OMI-DOAS differences for cloudy cases from −3% for low SZA to almost +2% for large SZA values. In general, we can say that the TOC data derived from the DOAS technique have a clear dependence on SZA for cloudy conditions. This behavior may be partially explained by the fact that the clouds influence on the ozone retrieval decreases with increasing SZA since the radiative transfer is dominated by absorption processes in the stratosphere rather than scattering-absorption processes in the troposphere for high SZA [*Koelemeijer and Stammes*, 1999]. On the other hand, the three curves for OMI-TOMS follow a similar pattern, showing a slight increase in underestimation as function of satellite SZA. Nevertheless, it can be seen that this underestimation presents a higher SZA dependence for cloud-free conditions than for cloudy cases.

[23] The other important viewing geometry parameter is the VZA or satellite scan angle. While GOME/ERS-2 instrument has only three scan positions between a VZA of −30° and +30°, its successor GOME-2/MetOp-A presents 24 positions between −60° and 60°. The SCIAMACHY instrument has 16 positions between a scan angle of −40° and +40°. The OMI ground swath has 2600 km of width, and it is divided into 60 ground pixels between a VZA of −63° and +63°, where positions 29 and 30 denote the exact "nadir" subsatellite positions with the smallest footprint [*Levelt*, 2002]. In Figure 2, the relative differences between Satellite and Brewer TOC data in the Iberian Peninsula are plotted as a function of the satellite scan angle. It can be seen that the positive scan angles (west pixels) for the two GOME instruments show a clear difference between the curves corresponding to cloud-free and cloudy cases. A larger difference between the cloud-free and cloudy curves can be observed for the SCIAMACHY instrument, mainly in the west pixels in correspondence with the two GOME instruments. Thus, the VZA dependence observed in GOME and SCIAMACHY instruments are very similar.

[24] Figure 2 shows that the relative differences derived from the OMI-DOAS algorithm present a slight dependence on satellite scan angle, mainly for cloud-free cases, but a large jump is observed around the OMI scan angle higher than +20° with a variation in the difference from −3% to +3%. The underestimation slightly increases as a function of the OMI scan angle from −63° to almost +20° observing then a clear change in the tendency for the extreme positions with an overestimation for cloud-free conditions. This result agrees with the pattern obtained for the other three DOAS retrieval algorithms; that is, they all have some issues for the

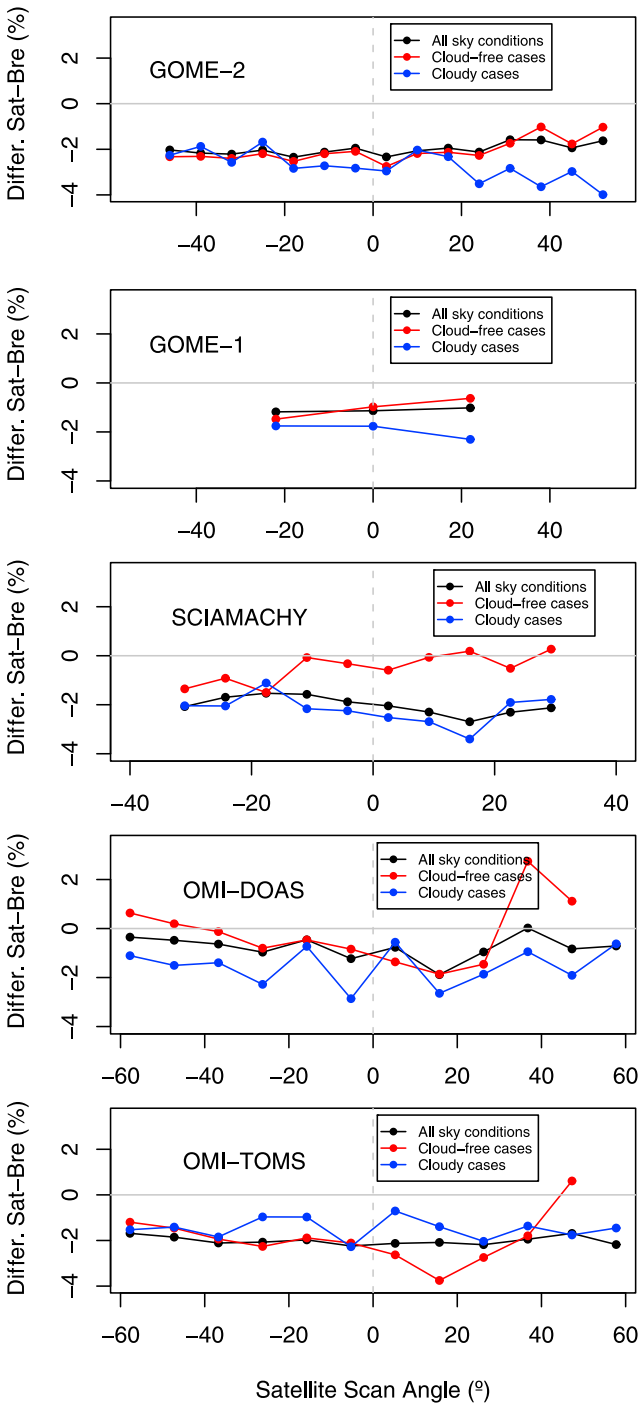

Figure 2. Dependence of satellite-Brewer relative differences with respect to the satellite scan angle for (top to bottom) GOME-2, GOME-1, SCIAMACHY, OMI-DOAS, and OMI-TOMS.

west pixels and cloud-free conditions. On the other hand, Figure 2 (bottom) shows that there is a very slight dependence of the differences between OMI-TOMS and Brewer TOC data with respect to the satellite scan angle for cloud-free conditions. This dependency is similar to the one found for OMI-DOAS, but with a more reduced amplitude. *Kroon et al.* [2008] and *Antón et al.* [2009b] indicated that the OMI TOC data retrieved by TOMS and DOAS algorithms are independent of swath position when all sky conditions are used together, i.e., without differencing cloud-free and cloudy cases. Figure 2 emphasize the need of separating effects of different sky and viewing geometry conditions over the satellite TOC data.

[25] Figures 3, 4, 5, and 6 examine the dependence of satellite–ground-based TOC differences on satellite cloud parameters, selecting cases with low (from 15° to 35°) and high (from 50° to 70°) SZA values. The cloud parameters play an important role in the calculation of the AMF and in the estimation of the "ghost" column hidden by the clouds to correct the shielding effect [*Van Roozendael et al.*, 2006; *Loyola et al.*, 2011]. Dependencies on TOC satellite data are analyzed with respect to the corresponding cloud properties used in their retrieval algorithms. Nevertheless, it is important to notice that the values of each cloud property for the different TOC satellite data are highly correlated, but they do not necessarily correspond to the same cloud conditions.

[26] Figure 3 shows the relative differences as a function of the cloud fraction (using bins of 10%) reported by the satellite retrievals. Each plot shows three curves corresponding to all, low and high SZA values. The dashed horizontal black line means the median value of the relative differences between the satellite and Brewer data for cloud-free conditions. It can be seen that for the four DOAS algorithms, the cases with high SZA values (blue curve) almost always present smaller underestimation of the ground-based data than the cases with low SZA values (red curve). This result is in agreement with Figure 1 where can be seen that DOAS algorithms present a significant positive dependence on SZA for cloudy cases. Clouds have a stronger influence on the satellite ozone retrieval for low SZA than for high SZA. In addition, it can be observed from Figure 3 that SCIAMACHY and OMI-DOAS algorithms have large amplitude between the curves corresponding to low and high SZA cases. In contrast, both GOME instruments show a more homogeneous pattern, especially for small and moderate CF. The GOME data sets also present a smooth, negative dependence with the CF values when all cases are considered. Nevertheless, GOME-2 shows a more stable behavior than GOME-1 which could be partially related to the fact that the GOME-2 footprint is 4 times smaller than the GOME-1 footprint The OMI-TOMS algorithm has a remarkable stability, showing no significant dependence on satellite CF for the three curves.

[27] Table 4 shows the median bias error (MBE) for all, cloud-free and cloudy conditions (see section 3) for each satellite data set. The reported errors correspond with the interquartile range (difference between the 75th and 25th percentile). It can be seen that MBE values for SCIAMACHY present a strong difference between cloud-free (−0.63%) and cloudy cases (−2.18%). In addition, GOME-1 and OMI-DOAS also shows a notable change from −0.74% (cloud-free cases) to −1.88 (cloudy cases), and from −0.42% to −1.38%, respectively. This behavior can be clearly seen in Figures 1–5 for these three algorithms. In contrast, GOME-2 and OMI-TOMS have large stability with slight variations from −2.00% to −2.46%, and from −1.91 to −1.55, respectively. The larger MBE cloud-free values for GOME-2 (−2.00%) compared to GOME-1 (−0.74%) may be attributed in part to remaining Level 1b radiometric calibration and

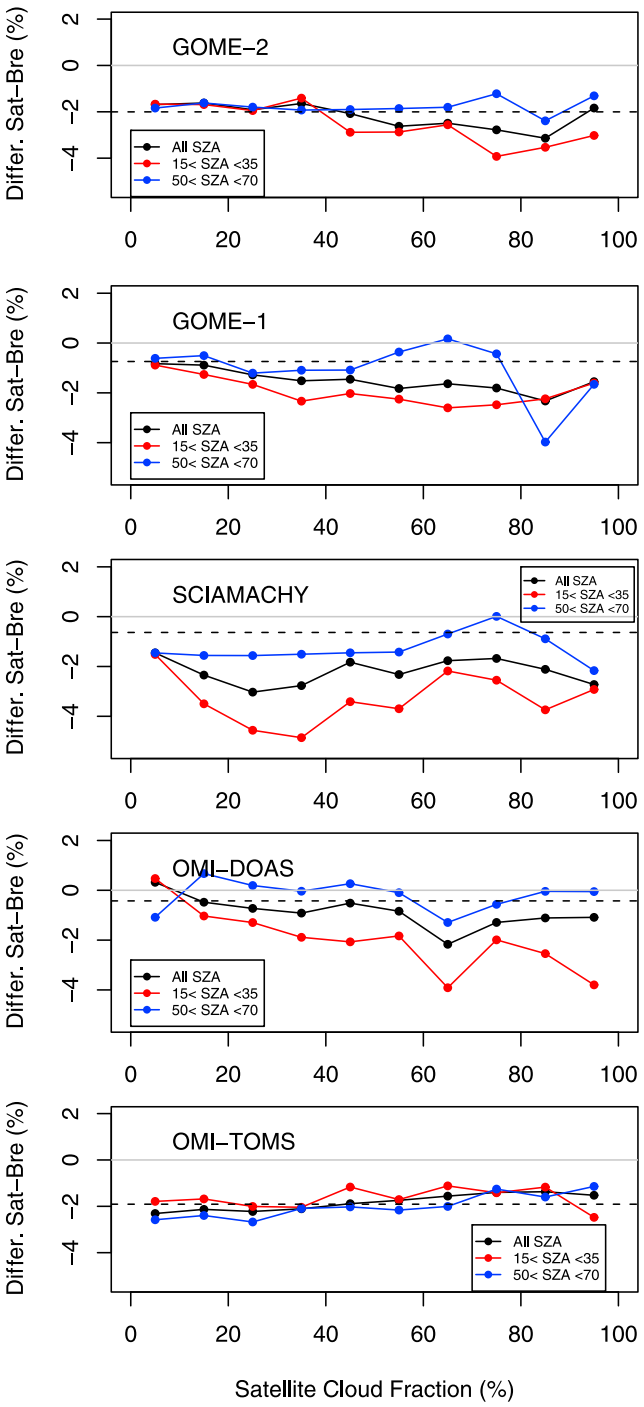

Figure 3. Evolution of the differences between total ozone column data retrieved by satellite (from top to bottom: GOME-2, GOME-1, SCIAMACHY, OMI-DOAS, and OMI-TOMS) and Brewer total ozone column data as function of satellite cloud fraction for all, low, and high solar zenith angles.

retrieval issues in the level 2 processing [*Balis et al.*, 2009]. From Table 4, it can be seen that the errors of the MBE values for cloudy cases are higher than for cloud-free cases, indicating that the scatter of the satellite-Brewer comparison is larger with increasing cloud fraction.

[28] The dependency of the relative differences with respect to the cloud top pressure for all, low and high SZA values is shown in Figure 4. It can be seen that GOME-1 and OMI-TOMS algorithms have the more stable behavior for the three curves, showing no significant dependence on CTP. The relative differences derived from the GOME-2

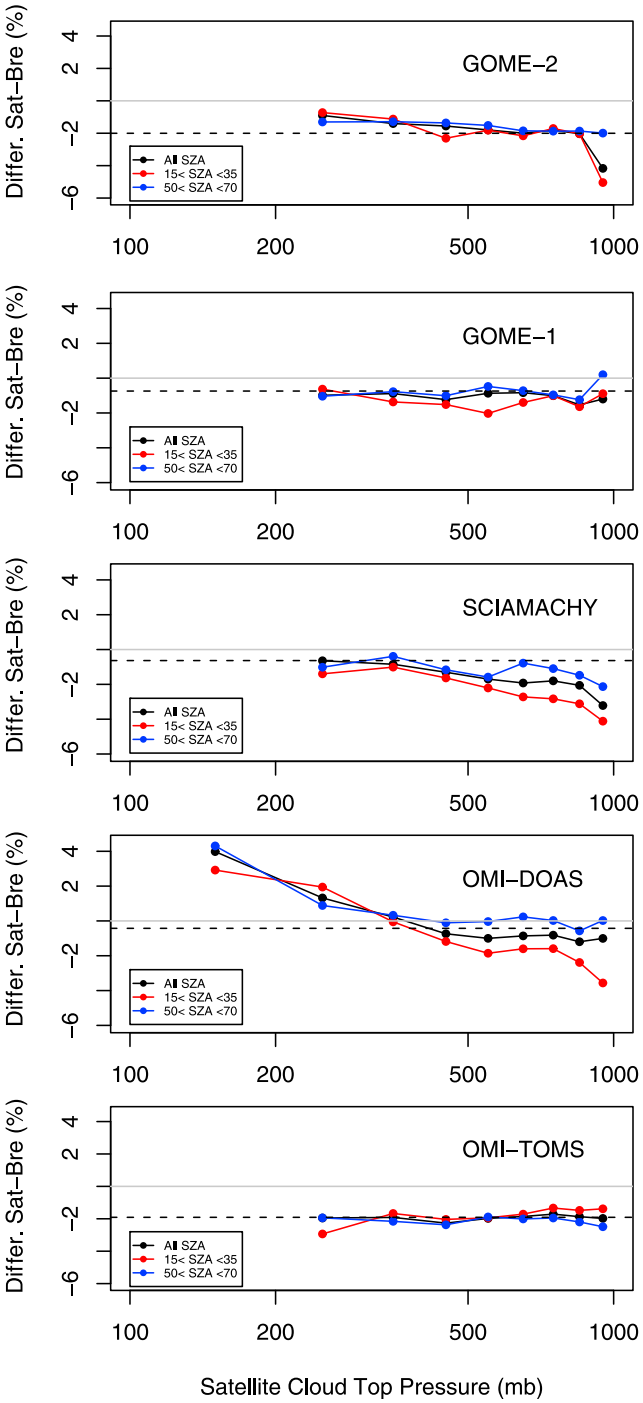

Figure 4. Evolution of the differences between total ozone column data retrieved by satellite (from top to bottom: GOME-2, GOME-1, SCIAMACHY, OMI-DOAS, and OMI-TOMS) and Brewer total ozone column data as function of satellite cloud top pressure for all, low, and high solar zenith angles.

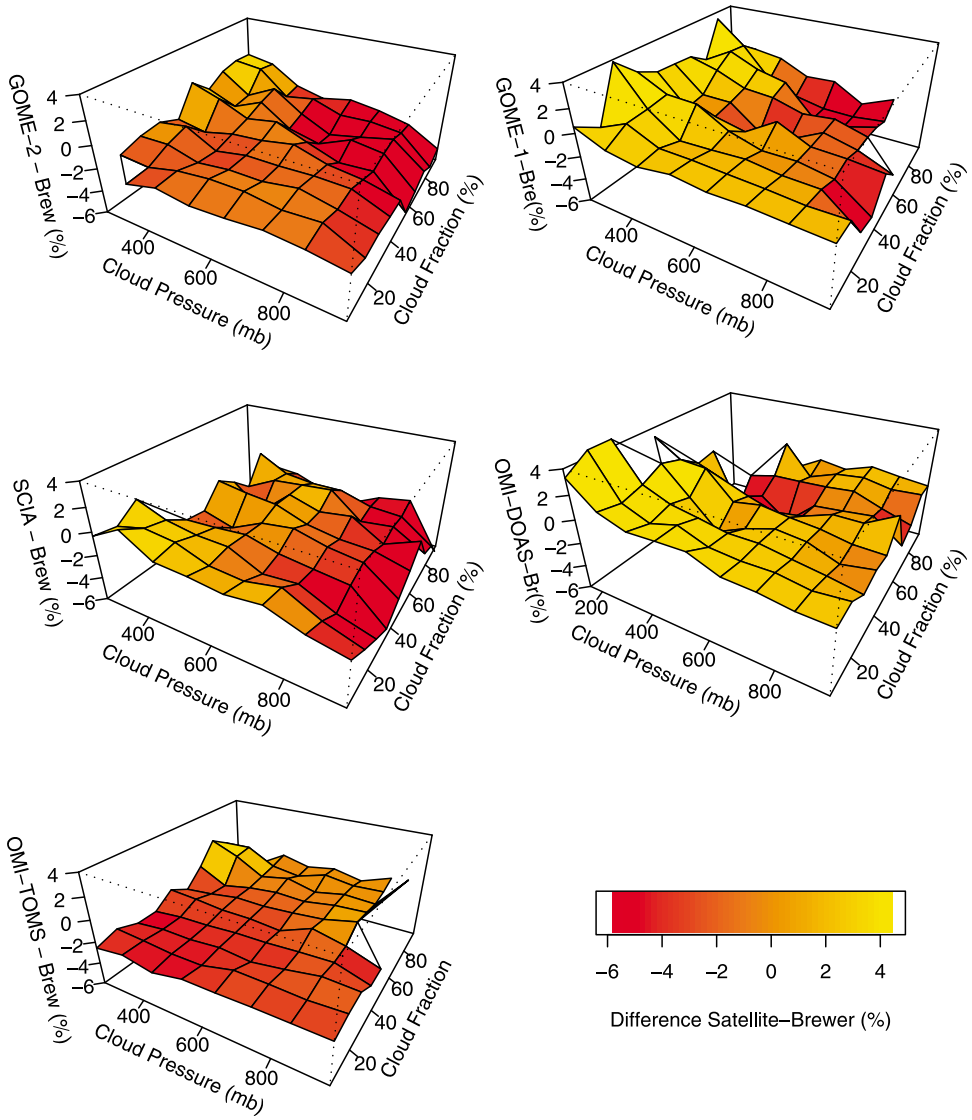

Figure 5. Evolution of the differences between total ozone column data retrieved by satellite (GOME-2, GOME-1, SCIAMACHY, OMI-DOAS, and OMI-TOMS) and Brewer total ozone column data as function of satellite cloud fraction and cloud top pressure.

algorithm present a stable pattern for all CTP values but a strong underestimation (~5%) for CTP values higher than 900 mbar (low clouds). The plot shows that this atypical behavior is caused by the low SZA values. The number of cases with CTP higher than 900 mbar are 28 (GOME-1), 133 (GOME-2), 805 (SCIAMACHY), 107 (OMI-TOMS), and 125 (OMI-DOAS). All satellite data sets present a realistic number of cases with low clouds except SCIAMACHY. This indicates that the FRESCO+ algorithm used to derive the cloud top pressure presents an evident uncertainty under low-cloud conditions. The CF values derived from all satellite instruments except SCIAMACHY have been selected for the days with very high SCIAMACHY CTP values (larger than 900 mbar). This analysis shows that the most of selected days are cloud-free cases. Therefore, many of the SCIAMACHY cases classified as low clouds really correspond to clear sky measurements.

[29] Figure 4 also shows that the satellite-Brewer differences obtained with the OMI-DOAS algorithm have a marked negative dependence with respect to the CTP, mainly for low SZA cases. Thus, for these cases, it can be observed a notable overestimation (~4%) for high clouds (CTP smaller than 200 mbar). These low CTP values have been only found in OMI-DOAS algorithm. The elevated overestimation could be related to the overestimation of the cloud top for these cases and the consequent overestimated "ghost" column added to the retrieved column amount for high clouds. For moderate-low clouds derived from the OMI-DOAS algorithm, the curve for high SZA values presents a stable behavior, while the low SZA values show a clear negative dependence with respect to the CTP. This last characteristic also appears in the SCIAMACHY plot, suggesting that these artifacts could be related to the usage of effective cloud parameters. In contrast, the satellite scan

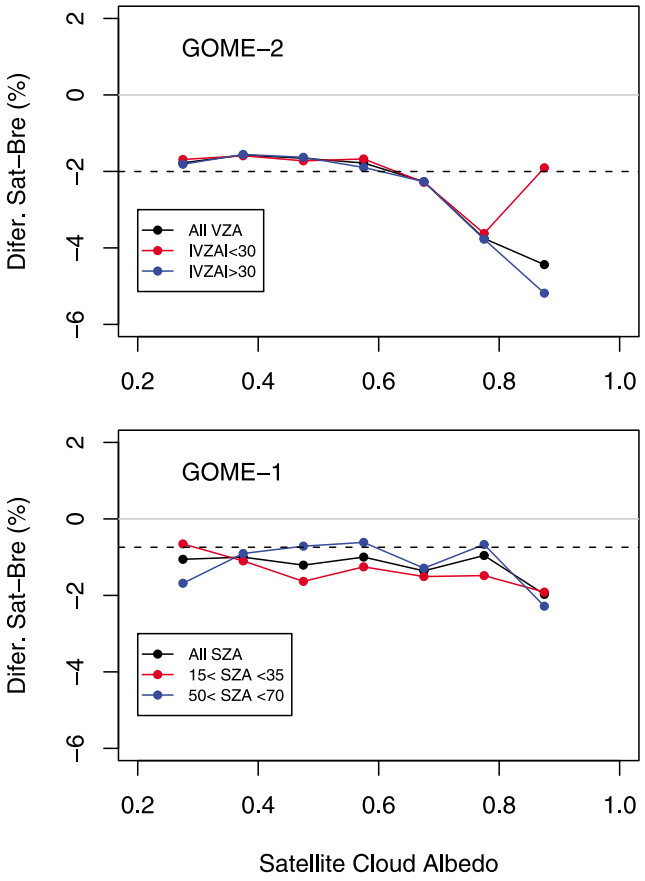

Figure 6. (top) Evolution of the differences between total ozone column data retrieved by (top) GOME-2 and (bottom) GOME-1 and Brewer total ozone column data as function of satellite cloud albedo for all, low, and high view zenith angles.

angle has no significant influence on the CTP dependence of the relative differences (not shown).

[30] It is interesting to analyze the concurrent influence of the CF and CTP parameters over the satellite-Brewer TOC differences. Figure 5 shows these relationships for each satellite data set. For GOME-2/MetOp-A, it can be seen that the high CF values are the main responsible of the strong underestimation obtained for low clouds (high CTP) shown in Figure 4. The same type of dependency explains the notable TOC underestimation obtained with SCIAMACHY for high CTP. The plot corresponding to GOME-1/ERS-2 in Figure 5 shows that there are not outliers with strong ozone underestimation for GOME-2/MetOp-A and SCIAMACHY. This plot confirms the stable behavior of GOME-1/ERS-2 data seen in Figure 4 even for high CTP values, which is not the case for GOME-2/MetOp-A and SCIAMACHY. On the other hand, the OMI-DOAS algorithm shows that the strong overestimation obtained for small CTP values (high clouds) is mainly associated with very small CF values (lower than 20%). When ozone retrieval errors induced by CTP uncertainties are analyzed, the albedo effect and the shielding effect have the same sign [*Koelemeijer and Stammes*, 1999]. Therefore even for small CFs an underestimation (overestimation) of CTP will cause an overestimation (underestimation) of the retrieved ozone column. Thus, the overestimation of Brewer TOC data obtained with the OMI-DOAS algorithm can be related to the underestimation of both CTP and CF parameters. The relative differences derived from the OMI-TOMS algorithm have a very stable behavior for all pairs of CF and CTP values with the exception of large CF values.

[31] Finally, the relationship between the relative differences and the cloud top albedo is studied in Figure 6 for GOME-2 (Figure 6, top) and GOME-1 (Figure 6, bottom). The other algorithms (SCIAMACHY, OMI-TOMS, and OMI-DOAS) use a fixed CTA of 0.8 and therefore it not possible to study the CTA influence on relative differences for these satellite algorithms. The differences derived from the GOME-1 instrument show no significant dependence on CTA for all, low and high SZA values. In contrast, the relative differences for GOME-2 present a notable underestimation (~5%) for high CTA values when all cases are considered. This underestimation is mainly caused by the satellite data during summer and autumn in the northern hemisphere (June to November) corresponding to scan angles (in absolute value) higher than 30° (not shown). Data during winter and spring do not present any scan angle dependency (not shown). The viewing scan angles for GOME-1 instrument are usually smaller than 30°. Figure 6 (top) shows that the cloud albedo dependence of GOME-2 ozone data even for scan angles smaller than 30° remains larger than for GOME-1 data set.

5. Conclusions

[32] We can draw a number of interesting conclusions from the detailed and systematic validation results of satellite TOC with Brewer data presented in this paper:

[33] 1. The influence of the cloud properties and viewing geometry parameters must be checked jointly since the interrelationship between them is very strong.

[34] 2. Generally speaking, the cloudiness that covers the satellite pixel (CF) causes a significant underestimation of the satellite TOC data compared with the cloud-free cases. The stronger underestimation is observed for SCIAMACHY data. For this instrument, the median relative differences with respect to Brewer data vary from −0.63% (cloud-free) to −2.18% (cloudy cases).

[35] 3. Regarding the dependency of the satellite-Brewer differences on SZA, the four DOAS algorithms show large dependences under cloudy conditions. The SCIAMACHY and OMI-DOAS are the data sets with larger variations (~3–4%) between low and high SZA for cloudy cases. These

Table 4. The Median Bias Error (MBE) for All, Cloud-Free, and Cloudy Conditions Corresponding to Each Satellite Algorithm[a]

	MBE All Cases (%)	MBE Cloud-Free (%)	MBE Cloudy (%)
GOME-2/MetOp-A	−1.95 ± 2.35	−2.00 ± 2.03	−2.46 ± 3.35
GOME/ERS-2	−1.10 ± 2.60	−0.74 ± 2.00	−1.88 ± 3.42
SCIAMACHY	−2.02 ± 3.30	−0.63 ± 2.39	−2.18 ± 3.63
OMI-DOAS	−0.69 ± 2.89	−0.42 ± 2.55	−1.38 ± 3.72
OMI-TOMS	−1.97 ± 1.84	−1.91 ± 1.39	−1.55 ± 2.53

[a]See section 3. The errors correspond with the interquartile range (difference between the 75th and 25th percentile).

systematic problems could be induced by the usage of effective cloud parameters in both retrievals. For the for DOAS algorithms, the satellite-Brewer differences clearly decrease with increasing SZA ass the clouds effects over the satellite ozone retrieval is considerable reduced for high SZA values. The OMI-TOMS data present a more stable SZA behavior which is partially explained by the large percentage of cloud-free cases (~57%) derived from the cloud algorithm used for this data set.

[36] 4. The dependences of the relative differences between the Brewer measurements and the satellite TOC data with respect to the cloud top pressure show that while the GOME-2 data present a strong underestimation for low clouds and high CF (~5%), the OMI-DOAS data show a very large overestimation for high clouds and low CF (~4%).

[37] 5. Finally, the GOME-2 data also present a strong underestimation (~5%) for cases with high cloud albedo values and large scan angles.

[38] All these results underline the importance of the precise treatment, modeling and estimation of cloud properties in order to obtain very accurate satellite TOC data.

[39] **Acknowledgments.** The authors would like to thank the teams responsible for the provision of satellite data used in this paper: the GOME-2/MetOp-A products were generated at DLR under the auspices of the O3MSAF project funded by EUMETSAT and national contributions, the SCIAMACHY/ENVISAT products were provided by BIRA, the GOME/ERS-2 products were generated at DLR under the auspices of the D-PAF project funded by ESA, and the OMI/AURA products were provided by the OMI International Team. The Brewer ozone data used in this study have been provided by the Spanish Agency of Meteorology (AEMET) (Madrid, Murcia, Zaragoza, and A Coruña) and the Spanish Institute of Aerospace Technique (INTA) (El Arenosillo). This work has been partially supported by Ministerio de Ciencia e Innovacion under project CGL2008-05939-C03-02/CLI. Manuel Antón thanks Ministerio de Ciencia e Innovación and Fondo Social Europeo for the award of a postdoctoral grant (Juan de la Cierva).

References

Ahmad, Z., P. K. Bhartia, and N. Krotkov (2004), Spectral properties of backscattered UV radiation in cloudy atmospheres, *J. Geophys. Res.*, *109*, D01201, doi:10.1029/2003JD003395.

Antón, M., D. Loyola, B. Navascúes, and P. Valk (2008), Comparison of GOME total ozone data with ground data from the Spanish Brewer spectroradiometers, *Ann. Geophys.*, *26*, 401–412, doi:10.5194/angeo-26-401-2008.

Antón, M., D. Loyola, M. López, J. M. Vilaplana, M. Bañón, W. Zimmer, and A. Serrano (2009a), Comparison of GOME-2/MetOp total ozone data with Brewer spectroradiometer data over the Iberian Peninsula, *Ann. Geophys.*, *27*, 1377–1386, doi:10.5194/angeo-27-1377-2009.

Antón, M., M. Lopez, J. M. Vilaplana, M. Kroon, R. McPeters, M. Bañón, and A. Serrano (2009b), Validation of OMI-TOMS and OMI-DOAS total ozone column using five Brewer spectroradiometers at the Iberian peninsula, *J. Geophys. Res.*, *114*, D14307, doi:10.1029/2009JD012003.

Antón, M., M. E. Koukouli, M. Kroon, R. D. McPeters, G. J. Labow, D. Balis, and A. Serrano (2010), Global validation of empirically corrected EP-TOMS total ozone columns using Brewer and Dobson ground-based measurements, *J. Geophys. Res.*, *115*, D19305, doi:10.1029/2010JD014178.

Balis, D., et al. (2007a), Ten years of GOME/ERS2 total ozone data: The new GOME Data Processor (GDP) version 4: 2. Ground-based validation and comparisons with TOMS V7/V8, *J. Geophys. Res.*, *112*, D07307, doi:10.1029/2005JD006376.

Balis, D., M. Kroon, M. E. Koukouli, E. J. Brinksma, G. Labow, J. P. Veefkind, and R. D. McPeters (2007b), Validation of Ozone Monitoring Instrument total ozone column measurements using Brewer and Dobson spectrophotometer ground-based observations, *J. Geophys. Res.*, *112*, D24S46, doi:10.1029/2007JD008796.

Balis, D., M. Koukouli, D. Loyola, P. Valks, and N. Hao (2009), Second validation report of GOME-2 total ozone products (OTO/O3, NTO/O3) processed with GDP4.2: Report of the Satellite Application Facility on Ozone and Atmospheric Chemistry Monitoring (O3M-SAF), *SAF/O3M/AUTH/GOME-2VAL/RP/02*, EUMETSAT, Darmstadt, Germany.

Basher, R. E. (1982), Review of the Dobson spectrophotometer and its accuracy, *Global Ozone Res. Monit. Proj. Rep. 13*, World Meteorol. Org., Geneva, Switzerland. (Available at http://www.esrl.noaa.gov/gmd/ozwv/dobson/papers/report13/report13.html)

Bhartia, P. K., and C. Wellemeyer (2002), TOMS-V8 total O3 algorithm, in *OMI Algorithm Theoretical Basis Document*, vol. II, *OMI Ozone Products*, edited by P. K. Bhartia, pp. 15–31, NASA Goddard Space Flight Cent., Greenbelt, Md. (Available at http://eospso.gsfc.nasa.gov/eos_homepage/for_scientists/atbd/index.php)

Bovensmann, H., J. P. Burrows, M. Buchwitz, J. Frerick, S. Noël, V. V. Rozanov, K. V. Chance, and A. P. H. Goede (1999), SCIAMACHY: Mission objectives and measurement modes, *J. Atmos. Sci.*, *56*, 127–150, doi:10.1175/1520-0469(1999)056<0127:SMOAMM>2.0.CO;2.

Bramstedt, K., J. Gleason, D. Loyola, W. Thomas, A. Bracher, M. Weber, and J. P. Burrows (2003), Comparison of total ozone from the satellite instruments GOME and TOMS with measurements from the Dobson network 1996–2000, *Atmos. Chem. Phys.*, *3*, 1409–1419, doi:10.5194/acp-3-1409-2003.

Burrows, J. P., et al. (1999), The Global Ozone Monitoring Experiment (GOME): Mission concept and first scientific results, *J. Atmos. Sci.*, *56*, 151–175, doi:10.1175/1520-0469(1999)056<0151:TGOMEG>2.0.CO;2.

Dobson, G. M. B. (1957), Observers' handbook for the ozone spectrophotometer, in *Annals of the International Geophysical Year*, vol. V, Part 1, pp. 46–89, Pergamon, New York.

Fioletov, V. E., J. B. Kerr, D. I. Wardle, N. I. Krotkov, and J. R. Herman (2002), Comparison of Brewer ultraviolet irradiance measurements with total ozone mapping spectrometer satellite retrievals, *Opt. Eng.*, *41*, 3051–3061, doi:10.1117/1.1516818.

Fioletov, V. E., J. B. Kerr, C. T. McElroy, D. I. Wardle, V. Savastiouk, and T. S. Grajnar (2005), The Brewer reference triad, *Geophys. Res. Lett.*, *32*, L20805, doi:10.1029/2005GL024244.

Kerr, J. B. (2002), New methodology for deriving total ozone and other atmospheric variables from Brewer spectrophotometer direct Sun spectra, *J. Geophys. Res.*, *107*(D23), 4731, doi:10.1029/2001JD001227.

Kerr, J. B., C. McElroy, and V. Evans (1984), The automated Brewer spectrophotometer, in *Proceedings of the Quadrennial Ozone Symposium*, edited by C. S. Zerefos and A. Ghazi, pp. 396–401, Am. Meteorol. Soc., Boston, Mass.

Koelemeijer, R. B. A., and P. Stammes (1999), Effects of clouds on ozone column retrieval from GOME UV measurements, *J. Geophys. Res.*, *104*, 8281–8294.

Kokhanovsky, A. A., and V. V. Rozanov (2008), The uncertainties of satellite DOAS total ozone retrieval for a cloudy sky, *Atmos. Res.*, *87*, 27–36, doi:10.1016/j.atmosres.2007.04.006.

Kokhanovsky, A. A., B. Mayer, V. V. Rozano, K. Wapler, L. N. Lamsal, M. Weber, J. P. Burrows, and U. Schumann (2007), The influence of broken cloudiness on cloud top height retrievals using nadir observations of backscattered solar radiation in the oxygen A-band, *J. Quant. Spectrosc. Radiat. Transfer*, *103*, 460–477, doi:10.1016/j.jqsrt.2006.06.003.

Komhyr, W. D. (1980), Operations Handbook—Ozone observations with Dobson spectrophotometer, *Global Ozone Res. and Monit. Proj. Rep. 6*, WMO, Geneva, Switzerland.

Krijger, J. M., M. van Weele, I. Aben, and R. Frey (2007), The effect of sensor resolution on the number of cloud-free observations from space, *Atmos. Chem. Phys.*, *7*, 2881–2891, doi:10.5194/acp-7-2881-2007.

Kroon, M., J. P. Veefkind, M. Sneep, R. D. McPeters, P. K. Bhartia, and P. F. Levelt (2008), Comparing OMI-TOMS and OMI-DOAS total ozone column data, *J. Geophys. Res.*, *113*, D16S28, doi:10.1029/2007JD008798.

Lerot, C., M. Van Roozendael, J. van Geffen, J. van Gent, C. Fayt, R. Spurr, G. Lichtenberg, and A. von Bargen (2009), Six years of total ozone column measurements from SCIAMACHY nadir observations, *Atmos. Meas. Tech.*, *2*, 87–98, doi:10.5194/amt-2-87-2009.

Levelt, P. F. (Ed.) (2002), *OMI Algorithm Theoretical Basis Document*, vol. I, *OMI Instrument, Level 0–1b Processor, Calibration and Operations*, 50 pp., NASA Goddard Space Flight Cent., Greenbelt, Md. (Available at http://eospso.gsfc.nasa.gov/eos_homepage/for_scientists/atbd/docs/OMI/ATBD-OMI-01.pdf)

Levelt, P. F., E. Hilsenrath, G. W. Leppelmeier, G. H. J. Van den Oord, P. K. Bhartia, J. Tamminen, J. F. De Haan, and J. P. Veefkind (2006), The Ozone Monitoring Instrument, *IEEE Trans. Geosci. Remote Sens.*, *44*(5), 1093–1101, doi:10.1109/TGRS.2006.872333.

Liu, X., M. J. Newchurch, R. Loughman, and P. K. Bhartia (2004), Errors resulting from assuming opaque Lambertian clouds in TOMS ozone retrieval, *J. Quant. Spectrosc. Radiat. Transfer*, *85*, 337–365, doi:10.1016/S0022-4073(03)00231-0.

Loyola, D., W. Thomas, Y. Livschitz, T. Ruppert, P. Albert, and R. Hollmann (2007), Cloud properties derived from GOME/ERS-2 backscatter data for trace gas retrieval, *IEEE Trans. Geosci. Remote Sens.*, *45*(9), 2747–2758.

Loyola, D., et al. (2011), The GOME-2 total column ozone product: Retrieval algorithm and ground-based validation, *J. Geophys. Res.*, doi:10.1029/2010JD014675, in press.

McPeters, R. D., et al. (1998), Earth Probe Total Ozone Mapping Spectrometer (TOMS) data products user's guide, *NASA Tech. Publ.*, *1998-206895*, 64 pp.

McPeters, R., M. Kroon, G. Labow, E. Brinksma, D. Balis, I. Petropavlovskikh, J. P. Veefkind, P. K. Bhartia, and P. F. Levelt (2008), Validation of the Aura Ozone Monitoring Instrument total column ozone product, *J. Geophys. Res.*, *113*, D15S14, doi:10.1029/2007JD008802.

Molina, M., D. Zaelke, K. M. Sarma, S. O. Andersen, V. Ramanathan, and D. Kaniaru (2009), Reducing abrupt climate change risk using the Montreal Protocol and other regulatory actions to complement cuts in CO2 emissions, *Proc. Natl. Acad. Sci. U. S. A.*, doi:10.1073/pnas.0902568106.

Morgenstern, O., P. Braesicke, M. M. Hurwitz, F. M. O'Connor, A. C. Bushell, C. E. Johnson, and J. A. Pyle (2008), The world avoided by the Montreal Protocol, *Geophys. Res. Lett.*, *35*, L16811, doi:10.1029/2008GL034590.

Munro, R., M. Eisinger, C. Anderson, J. Callies, E. Corpaccioli, R. Lang, A. Lefebvre, Y. Livschitz, and A. Perez Albinana (2006), GOME-2 on METOP: From in-orbit verification to routine operations, paper presented at Meteorological Satellite Conference, EUMETSAT, Helsinki, Finland.

Newchurch, M. J., X. Liu, J. H. Kim, and P. K. Bhartia (2001), On the accuracy of total ozone mapping spectrometer retrievals over tropical cloudy regions, *J. Geophys. Res.*, *106*, 32,315–32,326, doi:10.1029/2000JD000151.

Redondas, A., E. Cuevas, and A. Labajo (2002), Management and QA/QC of the Spanish Brewer spectrophotometer network, in *Sixth European Symposium on Stratospheric Ozone* [CD-ROM], edited by N. R. P. Harris, G. T. Amanatidis, and J. G. Levine, Comm. of the Eur. Commun., Göteborg, Sweden.

Redondas, A., et al. (2008), Second intercomparison campaign of the Regional Brewer Calibration Center-Europe, paper presented at Quadrennial Ozone Symposium, Eur. Comm., Tromso, Norway.

Rodriguez, D. G. L., W. Thomas, Y. Livschitz, T. Ruppert, P. Albert, and R. Hollmann (2007), Cloud properties derived from GOME/ERS-2 backscatter data for trace gas retrieval, *IEEE Trans. Geosci. Remote Sens.*, *45*(9), 2747–2758, doi:10.1109/TGRS.2007.901043.

Spurr, R., et al. (2005), GOME level 1-to-2 data processor version 3.0: A major upgrade of the GOME/ERS-2 total ozone retrieval algorithm, *Appl. Opt.*, *44*, 7196–7209, doi:10.1364/AO.44.007196.

Stammes, P., M. Sneep, J. F. de Haan, J. P. Veefkind, P. Wang, and P. F. Levelt (2008), Effective cloud fractions from the Ozone Monitoring Instrument: Theoretical framework and validation, *J. Geophys. Res.*, *113*, D16S38, doi:10.1029/2007JD008820.

Van Roozendael, M., et al. (2006), Ten years of GOME/ERS-2 total ozone data—The new GOME data processor (GDP) version 4: 1. Algorithm description, *J. Geophys. Res.*, *111*, D14311, doi:10.1029/2005JD006375.

Veefkind, J. P., J. F. de Haan, E. J. Brinksma, M. Kroon, and P. F. Levell (2006), Total ozone from the Ozone Monitoring Instrument (OMI) using the DOAS technique, *IEEE Trans. Geosci. Remote Sens.*, *44*, 1239–1244, doi:10.1109/TGRS.2006.871204.

Wang, P., P. Stammes, R. van der A, G. Pinardi, and M. van Roozendael (2008), FRESCO+: An improved O_2 A-band cloud retrieval algorithm for tropospheric trace gas retrievals, *Atmos. Chem. Phys.*, *8*, 6565–6576, doi:10.5194/acp-8-6565-2008.

World Meteorological Organization (WMO) (1996), Guide to meteorological instruments and methods of observation, 6th ed., *WMO Publ. 8*, Geneva, Switzerland.

World Meteorological Organization (WMO) (2006), Global ozone research and monitoring project, *Tech. Rep. 50*, Sci. Assess. of Ozone Depletion, Geneva, Switzerland.

M. Antón, Departamento de Física Aplicada, Universidad de Granada, E-18071 Granada, Spain. (mananton@unex.es)

D. Loyola, Remote Sensing Technology Institute, German Aerospace Center, Oberpfaffenhofen, D-82234 Wessling, Germany.